

Evaluation of the Impact of Having of Expansive Clay Core on the Stability of an Earth Dam

Kuo Chieh Chao¹, Faheem Shah¹, and Suttisak Soralump²

¹Department of Civil and Infrastructure Engineering, Asian Institute of Technology, Pathumthani, Thailand

²Department of Civil Engineering, Kasetsart University, Chatuchak, Bangkok, Thailand

E-mail: geoffchao@ait.ac.th

ABSTRACT: The study focuses on the changes in seepage and stability of the dam with a clay core constructed with expansive soils. Heave potential of the expansive clay core was also evaluated in the study. Laboratory testing was conducted to evaluate the swelling potential and hydraulic properties for the compacted expansive soils under various dry unit weights and initial water contents. Numerical modeling was conducted to evaluate the changes in seepage flow and slope stability due to the heaving of the expansive clay core for the dam. The findings suggest that to reduce seepage flow, the swelling soil should be compacted to a lower degree of compaction at a moisture content exceeding the optimum moisture content (OMC), which effectively reduces soil swelling and consequently minimizes seepage. Conversely, if stability is the primary concern, the swelling soil should be compacted to a relatively higher degree of compaction at a moisture content lower than the OMC, providing enhanced strength to the dam. In conclusion, the study demonstrates that for expansive soil used in dam cores, the same traditional compaction conditions utilized for seepage and stability in normal clayey soil can be applied. However, it is crucial to consider the specific characteristics of the swelling soil during the compaction process. By implementing suitable compaction techniques based on the desired outcome, seepage control, and dam stability can be effectively managed when utilizing swelling soil in dam construction. The findings offer valuable insights to engineers and practitioners involved in dam design and construction, aiding in informed decision-making and optimal compaction practices when incorporating swelling soils in dam cores.

KEYWORDS: Expansive clay core, Expansive soil, Seepage, Stability, Heave potential, and Time rate of heave.

1. INTRODUCTION

Expansive soil was used to construct the clay core of the Pa Sak Jolasid earth dam in Saraburi Province, Thailand. The hydraulic properties of the clay core could vary due to the heaving of the expansive clay. This research paper focuses on the seepage and slope stability analyses of the dam, specifically examining the influence of soil heaving on the soil water characteristics curve (SWCC) and unsaturated hydraulic conductivity function (K-function). Typically, dam seepage analyses do not take into account soil heaving when expansive soil is used for the construction of the dam. The SWCC and K-function used in these analyses are measured without considering soil heaving. This study aims to measure the SWCC and K-function while considering soil heaving in order to compare the resulting changes in seepage and slope stability of the dam.

General engineering practice is to compact the clay core material to 90 - 95% of the standard or modified Proctor dry density with a plus or minus percentage of the optimum moisture content (OMC). The extent of soil heaving varies depending on the initial soil compaction state. Therefore, this research also examines how the initial water content affects the seepage and stability of the dam, in addition to the factor of soil heaving. Moreover, the density of the clay core is an important factor as it affects the expansion of the expansive soil. Hence, the researcher aims to estimate the impact of soil density on the SWCC and k-function while evaluating the resulting changes in seepage and stability of the dam due to soil heaving.

Heaving of expansive soils could significantly affect the performance of infrastructures and foundations founded on expansive soils (Puppala et al., 2012; Bushra et al., 2017; Liu and Vanapalli, 2019; Shay et al., 2023). Heaving potential of the clay core constructed with expansive soils was also evaluated in the study. Heave potential calculations were conducted for soil samples compacted at various values of dry density and moisture content. The findings from this study will provide valuable insights into the complex interplay between soil heaving, SWCC, k-function, and dam seepage and stability, offering practical implications for dam construction and design.

2. MATERIAL PROPERTIES

In this research, soil samples were collected using PVC tubes from the Pa Sak Jolasid dam in Saraburi Province, Thailand. The samples were then transported to the laboratory for laboratory testing. After oven-drying, the samples were crushed to obtain smaller fine-grained soil particles. Sieve analyses were performed, and the soil particles passing through sieve no. 8 were selected for subsequent testing. The selection of the appropriate particle size was determined based on the desired sample size and the specific objectives of the study. The grain size distribution curve of the soil samples is presented in Figure 1. Table 1 provides an overview of the material properties of the soil samples, which served as a foundation for the subsequent investigation and analysis conducted in this study.

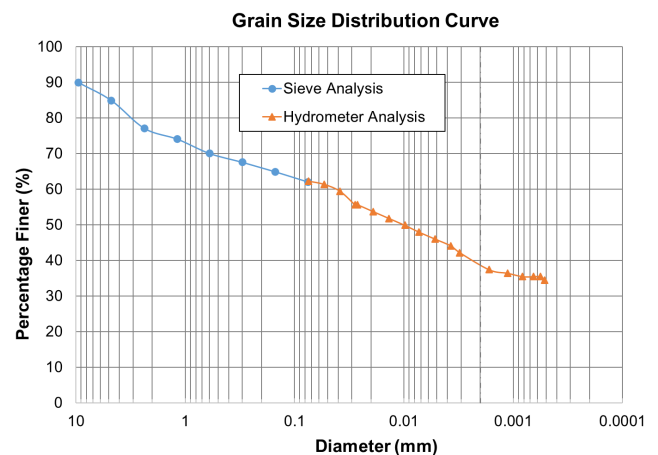


Figure 1 Grained size distribution curve

Table 1 Summary of material properties

Location	BH-2 (core zone)
Depth (m)	2 - 4
Percent passing sieve #200	62.08
Percent clay content	38
LL (%)	61.0
PL (%)	25.49
PI (%)	35.51
USCS	CH
OMC (%)	19
MDD (g/cm ³)	1.61

2.1 Swelling Potential

To further investigate the type of clay and its swelling potential, different approaches were used. Atterberg limits were combined with clay content to define a parameter called “Activity.” Skempton (1953) defined Activity (AC) as follows:

$$\text{Activity} = \frac{\text{Plasticity Index}}{\text{Percentage by weight finer than 0.002 mm}} \quad (1)$$

Table 2 shows the clay minerals and their typical activity values. Figure 2 presents the clay activity plot provided by Skempton (1953). The activity value obtained for the soil in this study was approximately 0.94. Using the values of the activity, clay content, and plasticity index of the soil, the soil was identified as very high activity “illite” based on the information presented in Table 2 and Figure 2. Furthermore, the soil was classified as high-plasticity clay (CH) using the Plasticity Chart. Tables 3 and 4 show the relationship between the Atterberg limits and swelling potential determined by Ola (1981) and Holtz and Bibbs (1956), respectively. The soil has a high swelling potential based on the relationships shown in Tables 3 and 4.

Table 2 Clay minerals and their typical activity values (Skempton, 1953)

Mineral	Activity
Kaolinite	0.33 - 0.46
Illite	0.9
Montmorillonite (Ca)	1.5
Montmorillonite (Na)	7.2

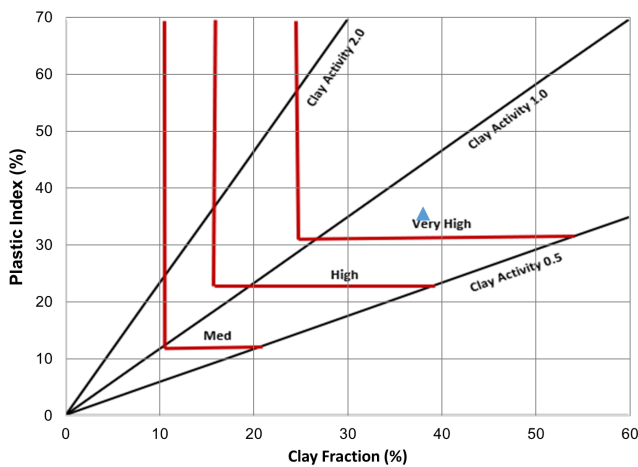


Figure 2 Activity plot of clay (Skempton, 1953)

It is also possible that Montmorillonite, a swelling clay mineral, is present in the soil based on the activity value (0.94) and the information provided in Table 2. To confirm the actual type of clay mineralogy of the soil, it is recommended to conduct X-ray diffraction (XRD) tests. The XRD analysis will provide detailed information about the mineral composition of the soil, allowing for a definitive determination of the clay mineralogy (Por et al., 2015).

Table 3 Plasticity index and swelling potential (Ola, 1981)

PI (%)	Swelling Potential
< 18	Low
15 - 28	Medium
25 - 41	High
> 35	Very high

Table 4 Liquid limits and swelling potential (Holtz and Bibbs, 1956)

LL (%)	Probable Expansion (%)	Swelling Potential
< 30	< 1	Low
30 - 40	1 - 5	Medium
40 - 60	3 - 10	High
> 60	> 10	Very high

2.2 Soil Water Characteristics Curve

Filter paper (FP) tests were employed in accordance with Chao et al. (1998 and 2008) to determine the SWCCs of the expansive soil. Soil samples were compacted to the desired bulk density (γ_d) and initial water content. The wetting SWCC curve was determined by wetting the soil with water. Two soil samples with similar volumetric water contents were selected for the FP tests. The Whatman No. 42 filter papers were used in the tests. The filter papers were placed between the soil specimens to measure the matric suction of the soil. The filter papers were also placed on top of the sample, separated by a small PVC ring between the filter papers and the soil sample, to measure the total suction of the soil. After seven days of moisture equilibrium, the top and bottom filter papers were quickly transferred to moisture-measuring tins, and their weights were measured. The filter papers were then dried in an oven, and their weights were measured again to calculate the water content.

The calibration curves published by ASTM D5298-16 and Chao (2007) were utilized to determine the SWCCs of the soil. The SWCCs were measured for soil samples compacted at various bulk densities (γ_d) and initial water contents, as indicated in Table 5. Figure 3 displays the SWCCs of the soil samples prepared at the maximum dry density (MDD), while Figure 4 illustrates the SWCCs of the soil specimens prepared at 95% of MDD.

Analysis of Figures 4 and 5 reveals that soil compacted at the dry optimum moisture content (OMC) exhibits greater swelling, resulting in lower volumetric water content compared to soils compacted at wet of OMC and optimum moisture content (Nelson et al., 2015). In other words, soil specimens compacted at higher initial water content demonstrate higher water retention capacity compared to those compacted at lower initial water content, as shown in Figures 4 and 5. Additionally, it is evident from Figures 4 and 5 that soil specimens compacted to maximum dry density (MDD) exhibit higher water retention capacity than those compacted at lower bulk densities. The soil specimens compacted at 95% of MDD display steeper slopes between 0.01 and 1 kPa soil suction compared to those compacted at MDD, indicating lower water-retention capacity (Gao and Sun, 2017 and Soundara et al., 2020). These findings highlight the influence of compaction conditions and initial water content on the soil water retention characteristics.

Table 5 Different initial compaction conditions of soil samples

Soil Samples	Initial Dry Density	Initial Water Content
SS1	1.61	17% (dry of opt.)
SS2	(MDD)	19% (opt.)
SS3		21% (wet of opt.)
SS4	1.53	17% (dry of opt.)
SS5	(95% of MDD)	19% (opt.)
SS6		21% (wet of opt.)

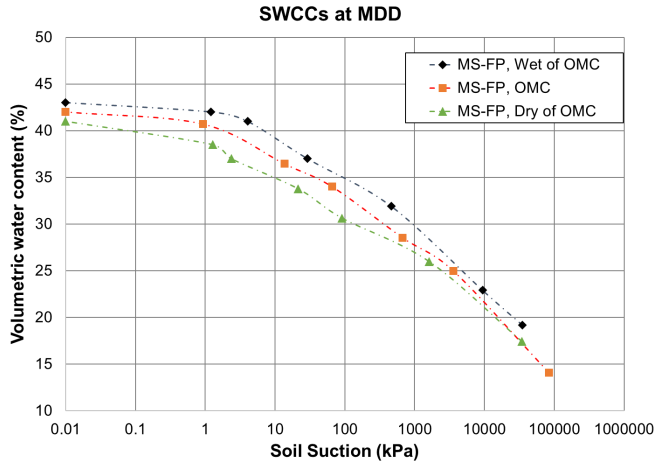


Figure 3 SWCCs at maximum dry density (1.61 g/cm³)

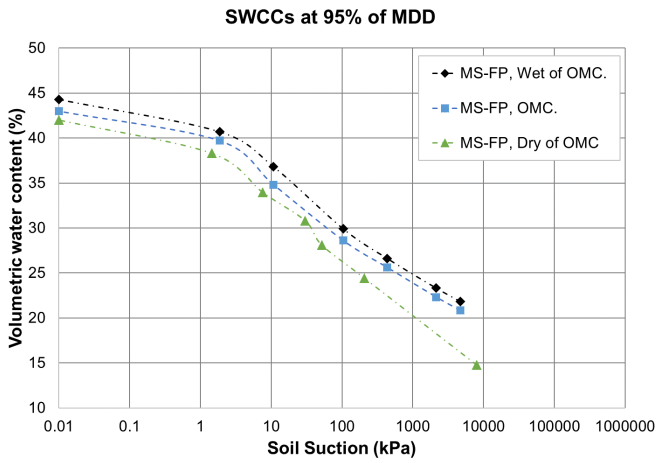


Figure 4 SWCCs at 95% of the maximum dry density

2.3 Unsaturated Hydraulic Conductivity Functions (K-functions)

The Fredlund-Xing-Huang (1994) approach was employed to estimate the K-function, which is crucial for understanding water seepage in unsaturated soil conditions. To estimate the K-functions using the Fredlund-Xing-Huang (1994) approach, the saturated hydraulic conductivity, K_{sat} , and the SWCC of the soil are needed. The results of the SWCCs of the soil were presented in the previous section. The K_{sat} measurement is described in this section.

The values of the saturated hydraulic conductivity of the expansive soil were determined using a flexible wall permeameter. The measured K_{sat} values are presented in Table 6. Table 6 shows that the soils compacted to dry of OMC have high saturated hydraulic permeability values compared to those compacted to wet of OMC. The reason is that at dry of OMC, the soil structure is flocculated, where there are more void spaces than soils compacted to wet of OMC where the compaction results in dispersed soil structure (Budhu, 2010). Furthermore, the soil compacted at MDD has lower permeability values as compared to the soil compacted at 95% of

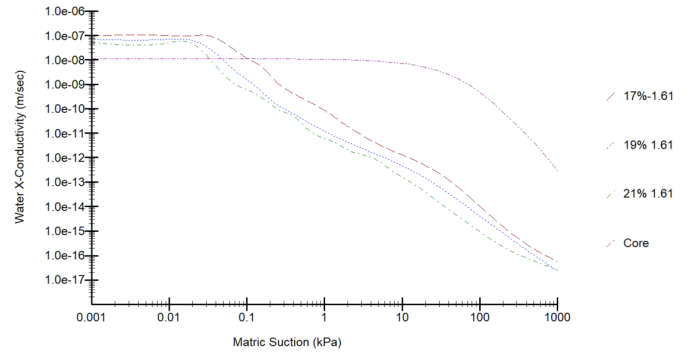
MDD due to the swelling of the soil. The soils compacted at dry of OMC will swell more as compared to wet of OMC. Thus, a high permeability value can be observed at dry of OMC.

To compare changes in seepage and stability of the dam with a clay core constructed with and without expansive soils, the soil sample was confined with an effective overburden pressure of 100 kPa, which is approximately equal to the measured value of the constant volume swelling pressure of 110 kPa for the soil. In theory, the soil will not swell under this pressure even when the soil is wetted (Nelson et al., 2003 and Nelson et al., 2017). The applied pressure resulted in a lower permeability value, as illustrated in Table 6, because the soil was prevented from swelling during the inundation process. The GeoStudio software was used to estimate the K-functions for each case using the corresponding k_{sat} (saturated hydraulic conductivity) values and the SWCCs of the soil. A comparison of the K-functions for various soil conditions is depicted in Figure 5.

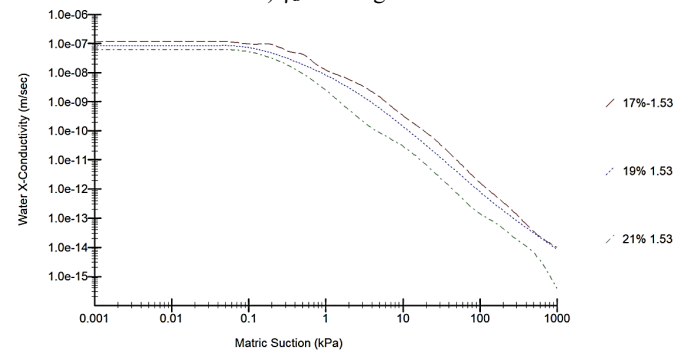
Table 6 Summary of shear strength parameters and saturated hydraulic conductivity values of soil specimens

Sample No.	Initial dry density (g/cm ³)	Initial water content (%)	Cohesion (kPa)	Friction angle (°)	K_{sat} (m/sec)
SS00*	1.61	17	25.58	26.33	1.11e-8
SS01		17	24.51	25.05	9.88e-8
SS02	1.61	19	23.14	23.30	6.90e-8
SS03		21	20.12	22.33	5.28e-8
SS04		17	22.15	24.23	1.13e-7
SS05	1.53	19	20.84	22.01	7.60e-8
SS06		21	17.98	19.59	6.89e-8

*Non-swelling soil as the soil was confined to prevent swelling



a) $\gamma_d = 1.61 \text{ g/cm}^3$



b) $\gamma_d = 1.53 \text{ g/cm}^3$

Figure 5 Unsaturated hydraulic conductivity functions: a) $\gamma_d = 1.61 \text{ g/cm}^3$ and b) $\gamma_d = 1.53 \text{ g/cm}^3$

2.4 Shear Strength Parameters

The direct shear test was performed in two steps for the expansive soil. First, the soil was consolidated for 24 hours under each normal

load. A slow shearing load was applied to shear the soil samples to avoid generating excessive pore water pressure. The normal loads for the expansive soil were selected based on the expected overburden stresses of 25, 50, and 100 kPa in the field. These normal loads were smaller than the constant volume swelling pressure of approximately 110 kPa for the soil, indicating that the soil would swell during consolidation. For comparison purposes, one soil sample (SS00) was subjected to normal loads greater than the constant volume swelling pressure, namely 100, 200, and 300 kPa. The soil exhibited no swelling during consolidation due to the normal loads exceeding the constant volume swelling pressure, σ'_{cv} . Similar to the other tests, slow shearing was performed after consolidation to prevent excess pore water pressure.

The shear strength parameters obtained from these tests are presented in Table 6. Table 6 shows that the soil specimens compacted at dry of OMC give higher shear strength values than those compacted at wet of OMC. The soils compacted to dry of OMC have lower water content. Therefore, it will have a flocculated structure (Budhu, 2010). The soil particles will have high inter-particle attractive forces in the flocculated structure. Thus, it will give a high cohesion value. While the soil compacted to wet of OMC will have more water, which results in a dispersed structure. Thus, the soil attractive forces will be less as compared to repulsive forces. In a dispersed structure, the attractive forces between soil particles are less, so it will have a smaller cohesion value. The soil sample prevented from swelling gives high shear strength compared to the swelling soils. The density of the soil reduces while the soil swells, and thus, the friction angle of the soil reduces after the swelling of the soil. The void ratio of the soil increases during the swelling process, and thus, water comes into the voids in the soil, which reduces the inter-particle attraction. Therefore, the cohesion of the soil reduces during the swelling process (Mahamedi and Khemissa, 2017; Tian et al., 2022).

2.5 Oedometer Tests

The oedometer tests are described in Nelson et al. (2015). There are two general types of oedometer tests, viz., the constant volume (CV) test and the consolidation-swell (CS) test. In the constant volume test, the sample is confined such that it cannot swell, and the stress required to prevent any swelling, i.e., to maintain a “constant value”, is termed the constant volume swelling pressure, σ'_{cv} . In the consolidation-swell test, a vertical stress is applied to the sample (the inundation pressure, σ'_i), and water is added to the sample. The amount by which the sample swells is termed the percent swell. Additional load is applied to the sample and the stress required to compress the sample to its initial thickness at which it was inundated is termed the consolidation-swell swelling pressure, σ'_{cs} . All tests were performed in general conformance with ASTM standard methods of test. Typical test results for both types of tests are shown in Figure 6 (Nelson et al., 2007a; Chao and Nelson, 2019).

2.5.1 Constant Volume (CV) Test

In the constant volume (CV) test, remolded soil specimens were prepared by compacting soil samples into floating rings with a diameter of 63.5 mm and a thickness of 20.5 mm. The soil specimens were formed in three layers using equal compaction energy for each layer. After compaction, two filter papers were placed, one at the top and the other at the bottom, while porous stones were positioned on top of the filter papers to facilitate the free flow of pore water. These prepared soil specimens were then placed in the GDS Automatic Oedometer System to conduct the CV tests. The top cap, attached to the machine’s loading frame, was securely fastened over the porous stone. A seating pressure of 6 kPa was applied for 5 minutes to stabilize the measurements.

Following the stabilization, the test proceeded by selecting the swelling option in the GDS Automatic Oedometer System, and water was introduced into the soil specimen. The specimen was maintained at a constant volume while incremental loads were applied to the sample. The test duration varied between 24 to 36 hours, depending

on the loading cell values. Once the loading cell values reached a steady state, the test was stopped, and the maximum pressure recorded by the loading cell was considered the constant volume swelling pressure, σ'_{cv} . The CV tests were conducted at an overburden stress of 24 kPa.

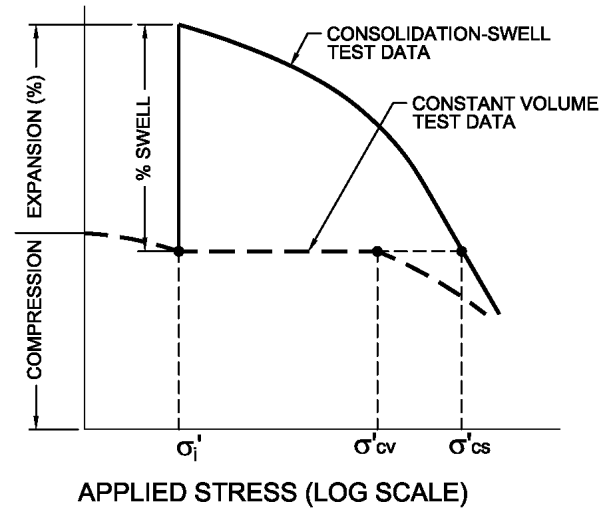


Figure 6 Oedometer test results

A total of six soil samples compacted at different initial water contents and dry densities, as shown in Table 5, were conducted in the CV tests. The results of the CV swelling pressures for each soil specimen were summarized in Table 7. Values of the depth of potential heave calculated using the measured CV swelling pressures are also presented in Table 7. The depth of potential heave is defined as the maximum depth where the constant volume swelling pressure is equal to the overburden pressure of the soil (Chao et al., 2006 & 2011; Nelson et al., 2015).

The research findings presented in Table 7 indicate that the CV swelling pressure of the soil specimen compacted at the maximum dry density (MDD) with lower water content is significantly higher compared to the specimen prepared at 95% of MDD. Moreover, an increase in the initial compaction water content corresponds to a decrease in the swelling pressure. These results emphasize that soils compacted at drier moisture levels result in greater swelling pressures. Additionally, higher initial dry densities during compaction lead to an increase in swelling pressure.

Table 7 Summary of CV swelling pressure and the corresponding depth of potential heave

Initial dry density (g/cm ³)	Initial water content (%)	CV swelling pressure (kPa)	Depth of potential heave (m)
1.53 (95% of MDD)	17	108.15	6.16
	19	102.31	5.73
	21	85.75	4.72
1.61 (MDD)	17	112.85	6.11
	19	106.82	5.69
	21	101.87	5.33

2.5.2 Consolidation-Swell (CS) Test

One soil sample compacted at the MDD of 1.61 g/cm³ with the optimum water content of 19% was conducted in the CS test. The sample was prepared following procedures similar to those described in the CV test section. The GDS Automatic Oedometer System was used for the test, and an inundation pressure of 6 kPa was applied in the CS test. The results of the CV test for the sample were summarized in Table 8. The results of the CV and CS test results were used in the heave prediction described in Section 4 of the paper.

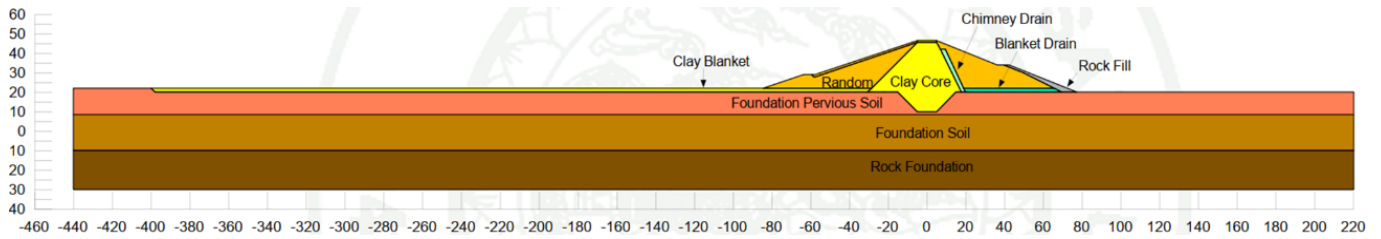


Figure 7 Pa Sak Jolasid dam cross-section (Naijit, 2022)

Table 8 Summary of CS swelling pressure

Initial dry density (g/cm ³)	Initial water content (%)	Percent swell (%)	CS swelling pressure (kPa)
1.61	19	5.4	189.6
(MDD)			

3. NUMERICAL MODELING

Numerical modeling was conducted to evaluate the changes in seepage and slope stability due to the heaving of the expansive clay core for the Pa Sak Jolasid earth dam in Saraburi Province, Thailand. Chao et al. (2014) indicated that modeling water migration in expansive soils is complex and challenging, and many factors need to be considered in doing such modeling. The numerical modeling conducted in this study only considered the changes in the hydraulic properties of the soil due to the heaving of the expansive soil.

The numerical analyses were conducted using the GeoStudio program (version 2022.1) under steady-state conditions. The software modules SEEP/W and SLOPE/W were employed for seepage and stability analyses, respectively.

3.1 Pa Sak Dam

Data including the cross-section and material properties obtained from Naijit (2022) was utilized in the numerical modeling. Figure 7 illustrates the cross-section of the dam, and Table 9 provides the material properties used in the analysis. This scenario aimed to assess how changes in compaction conditions and moisture content can affect the seepage and slope stability characteristics.

Table 9 Pa Sak Jolasid dam material properties (Modified from Naijit, 2022)

Material Type	γ_{sat} (kN/m ³)	k (m/s)	c' (kPa)	ϕ' (°)
Clay core	18.88	1.11e-8	25.58	26.33
Dam shell (Random)	18.00	3.67e-7	29.09	25.00
Filter drains	16.93	2.63e-5	0	35.00
Foundation doil	16.68	1e-7	11.00	36.70
Foundation pervious soil	22.00	1e-6	0	30.00

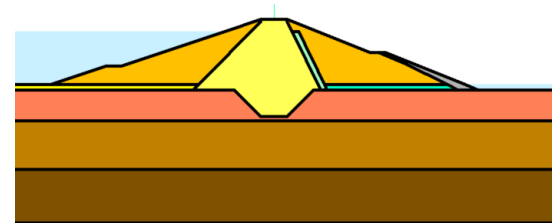
3.2 Reference Case

In order to investigate the influence of soil swelling on the dam's seepage and stability, different material configurations were considered for the clay core, while keeping the other materials constant, as outlined in Table 9. Figure 8 shows the scenarios analyzed in the study. The clay core was initially modeled as a non-swelling soil (designated as SS00 in Table 6), utilizing appropriate shear strength and permeability values to establish a reference case. The analysis procedure consisted of the following steps:

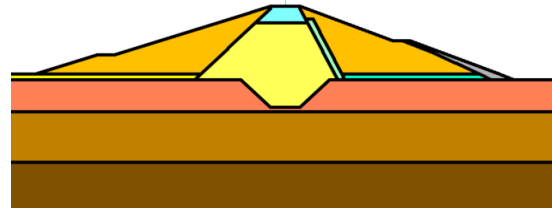
- 1) The dam geometry was accurately represented, and material properties were assigned to each soil layer. In the reference case, the clay core was considered non-swelling and represented by a single material (SS00).

- 2) Steady-state seepage analyses were performed under a maximum upstream head of 44.25 m, corresponding to the highest recorded water head during the 2010 flood in Thailand. This choice aimed to simulate a critical scenario for assessing the seepage behavior of the dam.
- 3) Subsequently, stability analyses were conducted using the results obtained from the seepage analyses.

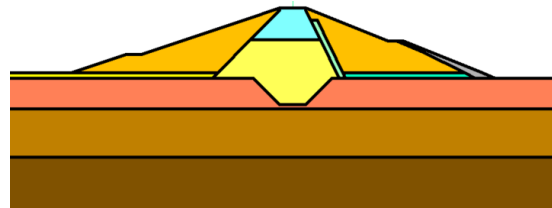
The seepage flow value for this model was determined to be 1.20688E-06 m³/sec, and the factor of safety (FOS) was determined to be 2.162, as illustrated in Figure 9.



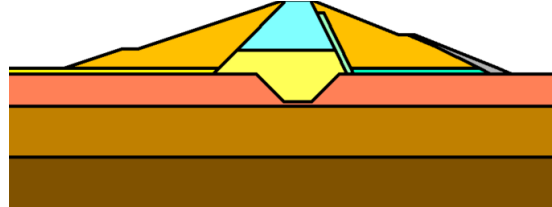
(a) Non-expansive clay core



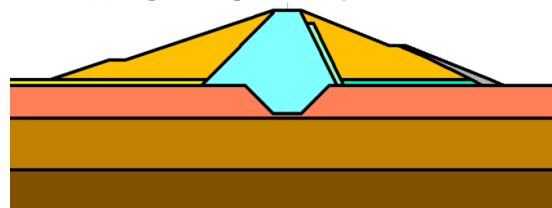
(b) Depth of expansive clay core = 6 m



(c) Depth of expansive clay core = 12 m



(d) Depth of expansive clay core = 18 m



(e) Depth of expansive clay core = 36 m

Figure 8 Scenarios of the expansive clay core with various heaving depths

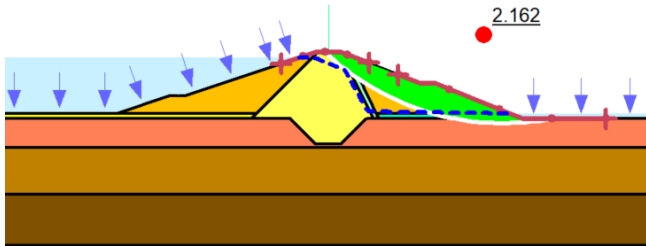


Figure 9 The factor of safety of reference non-swelling clay core at upstream water head = 44.25 m

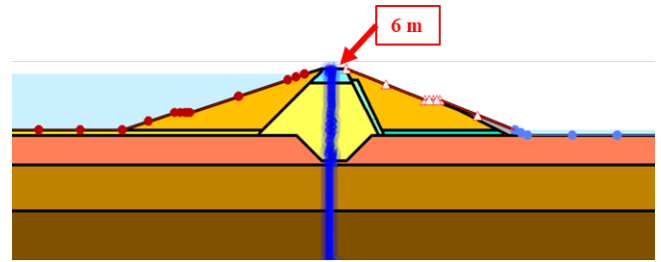


Figure 10 Top 6 m modified clay core in case of expansive clay core compacted at the maximum dry density to the dry of optimum moisture content

3.3 Effects of the Initial Water Content of Expansive Clay Core on Seepage and Slope Stability of the Dam

The extensive volume change associated with soil heaving can indeed impact both the density and SWCC of the soil. During heaving, the soil undergoes expansion, leading to a decrease in density. Additionally, as the soil swells, the capillary forces and suction change, affecting the water content at various suction levels. Consequently, the SWCC of heaving soil may exhibit variations compared to non-heaving soil (Chao et al., 2008). To account for these effects, soil properties such as density, SWCC, k-function, and shear strength parameters were measured after the occurrence of soil heaving. These properties measured after the swelling were used in the study to provide conservative estimations of the changes in the seepage and slope stability analyses.

In this study, the initial water content of the expansive soil was compacted at various values to examine the corresponding effects on seepage and slope stability of the dam. The soil specimens were compacted at three different water contents: dry of optimum moisture content (17%), optimum moisture content (19%), and wet of optimum moisture content (21%). The resulting depths of potential heave determined from the swelling pressures were measured as 6.11, 5.69, and 5.33 m for the samples with dry of OMC, OMC, and wet of OMC, respectively.

To incorporate the swelling behavior, specific modifications were made to the clay core of the dam based on the recorded swelling depths. The upper 6 m of the clay core was assigned with the SWCC and k-function derived from the expansive soil compacted at the maximum dry density (MDD) with dry of OMC, as shown in Figure 10. Additionally, the cohesion and internal angle of friction within this upper 6 m layer were replaced with the corresponding values obtained from the soil compacted at the MDD with dry of OMC (see Table 6). These same modifications were implemented for the cases involving expansive soil compacted at the OMC and wet of OMC. The recorded depths of potential heave for these cases were determined to be 5.69 m and 5.33 m, respectively.

Steady-state seepage and slope stability analyses were conducted to determine the seepage flow rate and FOS of the dam for each case. The results of the analyses are presented in Table 10. The results shown in Table 10 indicate a decrease in seepage from the dam as the initial water content of the compacted expansive clay core increases. Specifically, the case of the clay core compacted at the MDD with 17% initial water content (dry of OMC) exhibited the highest seepage rate of $1.2546 \times 10^{-6} \text{ m}^3/\text{sec}$. At the OMC case, the seepage rate decreased to $1.22088 \times 10^{-6} \text{ m}^3/\text{sec}$, and at wet of OMC case (21% initial water content), it further decreased to $1.22055 \times 10^{-6} \text{ m}^3/\text{sec}$. This corresponds to a percentage decrease in the seepage rate of 2.6% from dry of OMC and 2.7% from dry to wet of OMC.

Table 10 Summary of seepage flow rate and FOS

Initial dry density (g/cm^3)	Initial water content (%)	Total seepage rate (m^3/sec)	Factor of safety
1.61*	17	1.20688×10^{-6}	2.162
1.61	17	1.24610×10^{-6}	2.148
	19	1.22088×10^{-6}	2.142
	21	1.22025×10^{-6}	2.139
1.53	17	1.34097×10^{-6}	2.142
	19	1.23976×10^{-6}	2.139
	21	1.22846×10^{-6}	2.136

*Reference case: non-swelling soil as the soil was confined to prevent swelling

The reduction in the seepage rate can be attributed to two main factors. Firstly, when the soil is compacted to dry of OMC, it exhibits the highest swelling potential, resulting in a greater depth of potential heave of 6 m compared to 5.67 m and 5.41 m for the cases of optimum and wet of OMC, respectively. Consequently, the seepage is higher in the case of dry of OMC. Secondly, the structural fabric of the soil differs between the dry of OMC and wet of OMC cases. The soil compacted to dry of OMC demonstrates a flocculated structural fabric with a larger number of voids, while the soil compacted to wet of OMC exhibits a dispersed structure. As a result, the soil compacted at the 17% initial water content showed higher seepage than the soil compacted at the 21% initial water content, as depicted in Figure 11.

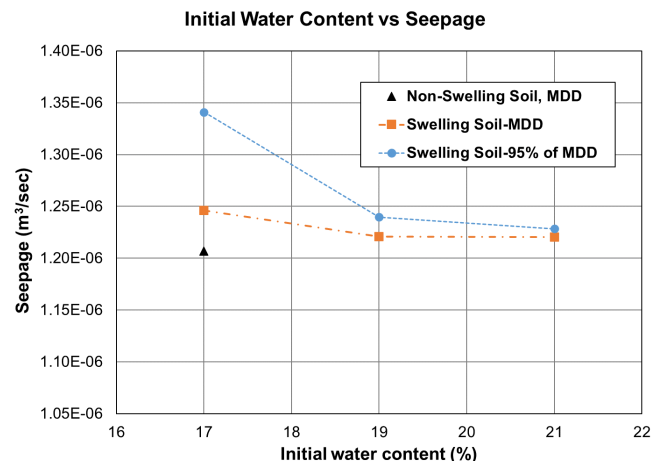


Figure 11 Seepage flow rate at different initial water contents

Figure 12 shows the effect of the expansive clay core with various heaving depths on the seepage rate. As indicated in Figure 12, the seepage flow rate increases as the heaving depth increases. The seepage rate could change significantly due to the heaving of the expansive clay core.

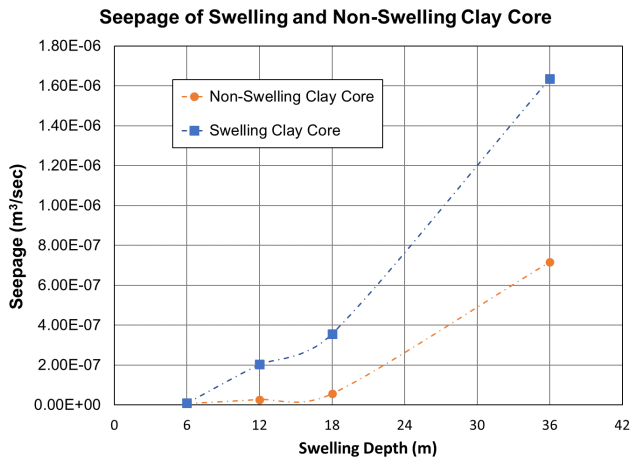


Figure 12 Seepage flow rate at different swelling depths

Figure 13 demonstrates that the factor of safety (FOS) at the dam downstream face decreases as the initial water content increases. The reduction in FOS can be attributed to two factors: the decrease in cohesion (c') and internal angle of friction (ϕ'), and the increase in seepage flow. Based on the previous discussion, the maximum decrease of 2.7% in seepage occurred from the dry of OMC to wet of OMC cases, which is not a significant change to impact the overall factor of safety. Therefore, in these cases, seepage does not significantly affect the overall factor of safety. Instead, the decrement in FOS can be attributed to a reduction in c' and ϕ' .

The highest factor of safety of 2.146 was observed at the dry of OMC case due to the clay core exhibiting higher shear strength parameters compared to the cases of OMC and wet of OMC. Specifically, the values of cohesion (c') and internal angle of friction (ϕ') at dry of OMC were measured as 24.51 kPa and 25.05 degrees, respectively. At the optimum water content, c' reduced to 23.14 kPa and ϕ' decreased to 23.30 degrees. Similarly, at the wet of OMC case, c' further reduced to 20.12 kPa and ϕ' decreased to 22.33 degrees. The shear strength of the soil plays a significant role in the overall factor of safety of the dam, as it provides the resisting strength to the sliding surface. Therefore, a reduction in the shear strength (τ_{shear}) of the soil results in a decrease in the resisting strength and consequently reduces the factor of safety.

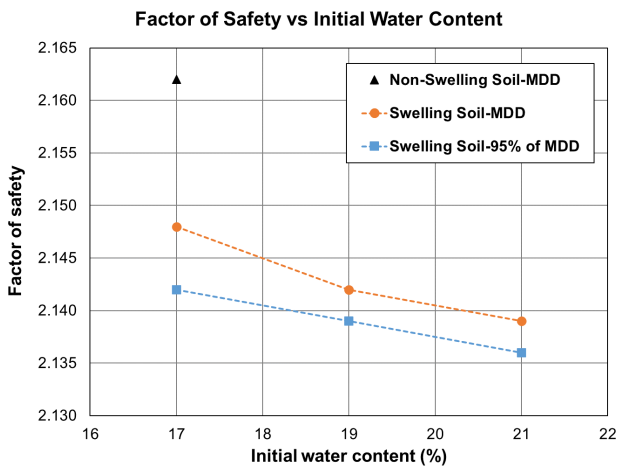


Figure 13 FOS at different initial water contents

Figure 14 shows the effect of the expansive clay core with various heaving depths on the factor of safety of the dam. As indicated in Figure 14, the factor of safety decreases as the heaving depth increases. The factor of safety of the dam could decrease by up to 2% in the cases analyzed.

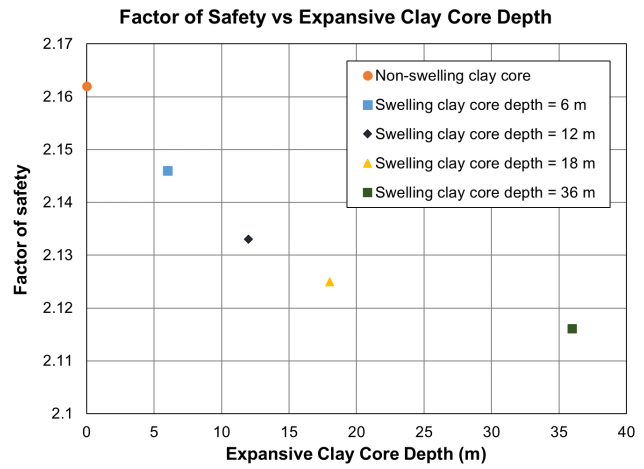


Figure 14 FOS at different expansive clay core depths

3.4 Effects of Initial Dry Densities of Expansive Clay Core on Seepage and Slope Stability of the Dam

The effect of expansive soils compacted to various initial dry density values on the seepage and slope stability of the dam was evaluated in this study. The results of the analyses are presented in Table 10 and Figure 11. It is evident in Figure 11 that the seepage flow rate increases with a decrease in the initial dry density (γ_d). Figure 11 also demonstrates that soils with different initial dry densities display different seepage flow rates despite having the same initial water content. Specifically, soils with lower initial dry densities result in higher seepage flow rates, while soils compacted to higher initial dry densities exhibit lower seepage flow rates. The percentage increases in seepage flow at the initial water contents of 17%, 19%, and 21% are 7.6%, 1.6%, and 0.6%, respectively, when the initial dry density decreases from the MDD (1.61 g/cm³) to 95% of the MDD (1.53 g/cm³).

The increase in seepage flow with decreasing initial dry density can be attributed to the increase in void spaces. When the soil is compacted at the same initial water content but with different initial dry densities, the soil with a lower initial dry density will possess more void spaces than the soil compacted at a higher initial dry density. Consequently, the seepage flow will be higher in the soil with a lower initial dry density than in the soil compacted at a higher initial dry density. It is important to note that both denser and lighter soils undergo swelling, leading to more voids and contributing to an overall increase in seepage flow. However, the denser soil demonstrates a greater swelling potential than the lighter soil while maintaining a lower void ratio, resulting in reduced seepage flow after swelling.

Furthermore, the seepage flow rate decreases as the initial water content increases. Soil compacted at dry of the optimum moisture content (OMC) exhibits a flocculated structural fabric with a greater number of voids than the dispersed structure observed in wet OMC. Consequently, the soil compacted at 17% initial water content displays higher seepage flow compared to the soil compacted at 21% initial water content. This trend holds for both initial dry density cases. The percentage decrease in seepage flow from dry to optimum water content when the soil is compacted at maximum dry density (MDD) is 2.6%, while the decrease from dry to wet of OMC is 2.7%. Similarly, for the soil compacted at 95% of the MDD, the percentage decrease in seepage flow from dry to optimum water content is 7.5%, while the decrease from dry to wet of OMC is 8.5%.

The factor of safety (FOS) for each case can be observed in Figure 13. The FOS is influenced by the degree of compaction, as shown in

Figure 13. Increasing the initial dry density leads to higher FOS values. This is attributed to the reduction in void spaces, which increases the soil's shear strength. Soils with a higher initial dry density exhibit higher FOS values at the same initial water content. For example, at 17% initial water content, a FOS of 2.146 was observed for the soil compacted at 1.61 g/cm³ (MDD), while a FOS of 2.142 was observed for the soil compacted at 1.53 g/cm³ (95% of MDD). Similar trends were observed at the 19% and 21% initial water content cases.

On the other hand, an increase in the initial water content results in a decrease in FOS at the dam's downstream face, as observed in Figure 13. This decrease can be attributed to the reduction in the shear strength and an increase in the seepage flow. The percentage decrease in the seepage flow from dry to wet of OMC was found to be relatively small. Therefore, the decrease in FOS is primarily related to the reduction in the shear strength. The highest FOS of 2.146 was observed for the soil compacted at the MDD with dry of OMC. When the soil was compacted at dry of OMC, the soil exhibited a higher shear strength compared to the soils compacted at the optimum and wet of OMC.

4. HEAVE PREDICTION

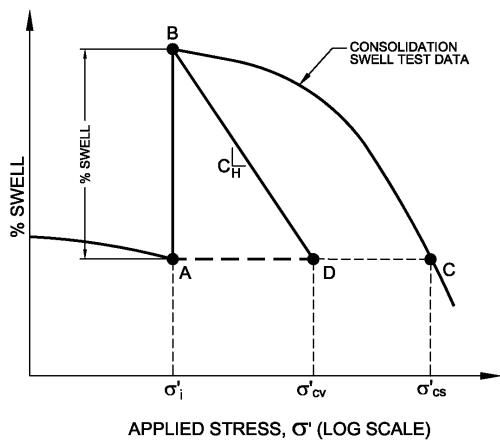
The equation for computing heave is (Nelson et al., 2015),

$$\rho = C_H \Delta z \log \left(\frac{\sigma'_{cv}}{\sigma'_f} \right) \tag{2}$$

Where:

- ρ = the amount of heave,
- Δz = the thickness of the soil layer for which heave is being computed,
- σ'_{cv} = the CV swelling pressure,
- σ'_f = the vertical stress at the midpoint of the soil layer for the conditions under which heave is being computed, and
- C_H = the heave index of the soil, a parameter that will be discussed below.

The term C_H represents a relationship between the percent swell (%S) that will occur in a sample of soil, and the vertical stress applied at the time of inundation. As such, it is not the slope of a stress-strain curve but must be developed from two or more oedometer tests. For purposes of discussion, it is convenient to consider the test results for a consolidation-swallow test and for a constant-volume test, as shown in Figure 15.



DETERMINE OF HEAVE INDEX
Figure 15 Determination of heave index C_H

In the constant-volume test, the percent swell corresponding to the particular value of σ'_i shown is percent swell (%S). At an inundation pressure of σ'_{cv} the percent swell would be zero. Thus, points B and D fall on the line representing the desired relationship

between σ'_i and %S. If it is assumed that this relationship is represented by a straight line on a semi-logarithmic plot, the line BD will represent the desired relationship. The parameter C_H is the slope of that line. Therefore,

$$C_H = \frac{\%S}{\log \sigma'_{cv} - \log \sigma'_i} = \frac{\%S}{\log \left(\frac{\sigma'_{cv}}{\sigma'_i} \right)} \tag{3}$$

To facilitate the use of Equation (3) and to determine both %S and σ'_{cv} from a single oedometer test, a relationship has been developed between σ'_{cs} and σ'_{cv} so that the constant volume swelling pressure, σ'_{cv} , can be determined from the CS oedometer test. A number of investigators have proposed relationships between σ'_{cv} and σ'_{cs} (Reichler, 1997; Bonner, 1998; Thompson et al., 2006; Nelson et al., 2006 and 2012; Nelson et al., 2007b). Nelson and Chao (2014) proposed the following equation for the relationship between σ'_{cs} and σ'_{cv} .

$$\log \sigma'_{cv} = \frac{\log \sigma'_{cs} + m \log \sigma'_i}{1 + m} \tag{4}$$

The parameter, m, depends on the particular soil, its expansive nature, and other properties of the soil. Nelson and Chao (2014) concluded that the values of m for the clay and the claystone samples range from 0.1 to 1.8, with an average value of 0.7.

The m value for the sample compacted at the MDD of 1.61 g/cm³ with the optimum water content of 19% using the data shown in Tables 7 and 8 and Equation (4) was calculated to be 0.2. This value is in the general range of the m values obtained in Nelson and Chao (2014). The m value was used in the heave calculations described below.

The total heave prediction was conducted for the samples compacted at the MDD of 1.61 g/cm³ with the water contents of 17% (dry of OMC), 19% (OMC), and 21% (dry of OMC) using Equation (2). The calculated values of the total heave for the cases were summarized in Table 11. As shown in Table 11, the total heave potential ranges from 99.1 to 111.8 mm, depending on the initial compaction efforts. The rule of thumb in geotechnical engineering practice is to assume that the differential heave is equal to half of the total heave. Therefore, the differential heave for the site could range from 49.6 to 55.9 mm, which exceeds the common allowable differential heave of 25 mm for structures.

Table 11 Summary of total heave prediction

Initial dry density (g/cm ³)	Initial water content (%)	CV swelling pressure (kPa)	$C_H^{(1)}$	Predicted total heave (mm)
1.61	17	112.85	--	111.8
(MDD)	19	106.82	0.043	104.1
	21	101.87	--	99.1

Note: (1) calculated using Equation (3) for the sample compacted at the MDD of 1.61 g/cm³ with the optimum water content of 19%.

5. CONCLUSIONS

For ordinary non-expansive soils, the general geotechnical practice is to compact the soil to 90 - 95% of the standard or modified Proctor dry density with a plus or minus percentage of the optimum moisture content. However, it is concluded from this study that when expansive soil is used, it is recommended to compact the soil at a lower density and to the wetter side of the OMC. Moreover, the results of the study indicated that the use of expansive soils for the clay core could increase seepage flow significantly through the earth dam. The change in the flow rate depends on factors such as the degree of compaction and the swelling potential of the soil.

The research emphasized that the slope stability of the dam was compromised when the normal clay core was replaced with expansive soil. The reduction in slope stability was particularly significant

when the expansive soil was wetted, and thus, the shear strength of the soil was reduced. For instance, if the entire 36 m of the non-expansive clay core were replaced with expansive clay, the FOS decreased from 2.162 to 2.117. Furthermore, compacting the soil to the wet of the optimum moisture content also reduced slope stability. These reductions in stability can be attributed to a decrease in shear strength parameters associated with soil swelling. This further emphasizes the importance of carefully evaluating the implications of using expansive soils in dam construction and the need for appropriate mitigation measures.

The total heave potential of the expansive clay core was computed to range from 99.1 to 111.8 mm, depending on the initial compaction efforts. The differential heave for the site could range from 49.6 to 55.9 mm if it is assumed that the differential heave is approximately equal to half of the total heave. The predicted differential heave could exceed the common allowable differential heave of 25 mm for structures. It is suggested that the actual differential heave profile of the dam be evaluated using numerical model method, as described in Chao et al. (2017).

The findings provide valuable insights for engineers and practitioners involved in geotechnical engineering projects, particularly those dealing with expansive soils. By providing appropriate compaction requirements of expansive soils, engineers can make well-informed decisions to reduce swelling, control seepage, and ensure the long-term stability of dam structures.

6. REFERENCES

- ASTM. D5298-16. (2016). "Standard Test Method for Measurement of Soil Potential (Suction) Using Filter Paper." *ASTM International: West Conshohocken, PA*.
- Bonner, J. P. (1998). "Comparison of Predicted Heave using Oedometer Test Data to Actual Heave." *MS Thesis, Colorado State University, Fort Collins, Colorado*.
- Budhu, M. (2010). "Soil Mechanics and Foundations." *3rd Edition, John Wiley & Sons Inc., Hoboken*.
- Bushra, S. A., Safa, H. A. A., and Hassan, O. A. (2017). "Numerical Modelling of Retaining Wall Resting on Expansive Soil." *Geotechnical Engineering Journal of the Southeast Asian Geotechnical Society and Association of Geotechnical Societies in Southeast Asia*, 48(4), December.
- Chao, K. C. (2007). "Design Principles for Foundations on Expansive Soils." *Ph.D. Dissertation, Colorado State University, Fort Collins, CO*.
- Chao, K. C. and Nelson, J. D. (2019). "Validation of Foundation Design Method on Expansive Soils." *Geotechnical Engineering Journal of the Southeast Asian Geotechnical Society and Association of Geotechnical Societies in Southeast Asia*, 50(1), March.
- Chao, K. C., Durkee, D. B., Miller, D. J., and Nelson, J. D. (1998). "Soil Water Characteristic Curve for Expansive Soils" *Thirteenth Southeast Asian Geotechnical Conference, Taipei, Taiwan*. November.
- Chao, K. C., Kang, J. B., and Nelson, J. D. (2014). "Challenges in Water Migration Modeling for Expansive Soils." *GeoShanghai Conference, Shanghai, China*.
- Chao, K. C., Kang, J. B., and Nelson, J. D. (2018). "Evaluation of Failure of Embankment Slope Constructed with Expansive Soils." *Geotechnical Engineering Journal of the Southeast Asian Geotechnical Society and Association of Geotechnical Societies in Southeast Asia*, 49(2), June. 140-149.
- Chao, K. C., Nelson, J. D., and Overton, D. D. (2011). "Factors Influencing Design of Deep Foundations on Expansive Soils." *The Fifth Asia-Pacific Conference on Unsaturated Soils, Pattaya, Thailand*.
- Chao, K. C., Nelson, J. D., Overton, D. D., and Cumbers, J. M. (2008). "Soil Water Retention Curves for Remolded Expansive Soils." *Proceedings of the 1st European Conference on Unsaturated Soils, Durham, UK*.
- Chao, K. C., Overton, D. D., and Nelson, J. D. (2006). "Design and Installation of Deep Benchmarks in Expansive Soil." *Journal of Surveying Engineering, American Society of Civil Engineers*, 132(3), 124-131.
- Fredlund, D. G., and Xing, A. (1994). "Equations for the Soil-Water Characteristic Curve." *Canadian Geotechnical Journal*, 31(3), 521-532.
- Gao, Y., and Sun, D. (2017). "Soil-Water Retention Behavior of Compacted Soil with Different Densities Over a Wide Suction Range and its Prediction." *Computers and Geotechnics*, 91, 17-26. 10.1016/j.compgeo.2017.06.016.
- Holtz, W. G., and Gibbs, H. J. (1956). "Engineering Properties of Expansive Clays." *Transactions ASCE*, 121, 641-677.
- Liu, Y. and Vanapalli, S. K. (2019). "Simplified Shear Deformation Method for Analysis of Mechanical Behavior of a Single Pile in Expansive Soils." *Geotechnical Engineering Journal of the Southeast Asian Geotechnical Society and Association of Geotechnical Societies in Southeast Asia*, 50(1), March.
- Mahamedi, A. and Khemissa, M. (2017). "Shear Strength of an Expansive Overconsolidated Clay Treated with Hydraulic Binders." *Geotechnical Engineering Journal of the Southeast Asian Geotechnical Society and Association of Geotechnical Societies in Southeast Asia*, 48(4), December.
- Morin, W. J., and Todor, P. C. (1976). "Laterite and Lateritic Soils and Other Problem Soils of the Tropics." *Lyon Associates, Baltimore & Road Research Institute, Rio de Janeiro, USAID/csd 3682, Instruction Manual*, 2, 92.
- Naijit, K. (2022). "Stability of Pasak Jolasid Dam Affected from Dry and Wet Cycles of Swelling Embankment Soil." *Master Thesis, Kasetsart University, Bangkok, Thailand*.
- Nelson, E. J., Chao, K. C., Nelson, J. D., and Overton, D. D. (2017). "Lessons Learned from Foundation and Slab Failures on Expansive Soils." *Journal of Performance of Constructed Facilities*. ASCE, 31(3).
- Nelson, J. D., and Chao, K. C. (2014). "Relationship Between Swelling Pressures Determined by Constant Volume and Consolidation-Swell Oedometer Tests." *Proceedings of the Sixth International Conference on Unsaturated Soils, Unsat., Sydney, Australia*.
- Nelson, J. D., Chao, K. C., and Overton, D. D. (2007a). "Design of Pier Foundations on Expansive Soils." *Proceedings of the 3rd Asian Conference on Unsaturated Soils, Nanjing, China*. April.
- Nelson, J. D., Chao, K. C., and Overton, D. D. (2007b). "Definition of Expansion Potential for Expansive Soil." *Proceedings of the 3rd Asian Conference on Unsaturated Soils, Nanjing, China*. April.
- Nelson, J. D., Chao, K. C., Overton, D. D., and Nelson, E. J. (2015). "Foundation Engineering for Expansive Soils." *John Wiley & Sons, Inc., New York, NY*.
- Nelson, J. D., Chao, K. C., Overton, D. D., and Schaut, R. W. (2012). "Calculation of Heave of Deep Pier Foundations." *Geotechnical Engineering Journal of the Southeast Asian Geotechnical Society and Association of Geotechnical Societies in Southeast Asia*, 43(1), 12-25.
- Nelson, J. D., Overton, D. D., and Chao, K. C. (2003). "Design of Foundation for Light Structures on Expansive Soils." *California Geotechnical Engineers Association, 2002-2003 Annual Conference, Carmel, California, USA*. April.
- Nelson, J. D., Reichler, D. K., and Cumbers, J. M. (2006). "Parameters for Heave Prediction by Oedometer Tests." *Proceedings of the 4th International Conference on Unsaturated Soils, Carefree, Arizona*. 951-961.
- Ola, S.A. (1983). "Tropical Soils of Nigeria in Engineering Practice." *A.A. Balkema/Rotterdam Edition, Netherlands*.
- Por, S., Likitlersuang, S., and Nishimura, S. (2015). "Investigation of Shrinkage and Swelling Behaviour of Expansive/Non-Expansive Clay Mixtures." *Geotechnical Engineering Journal of the Southeast Asian Geotechnical Society and Association of Geotechnical Societies in Southeast Asia*, 46(1), March.
- Puppala, A. J., Wejrungsikul, T., Puljan, V., and Manosuthikij, T. (2012). "Measurements of Shrinkage Induced Pressure (Sip) in

- Unsaturated Expansive Clays.” *Geotechnical Engineering Journal of the Southeast Asian Geotechnical Society and Association of Geotechnical Societies in Southeast Asia*, 43(1), March.
- Reichler, D. K. (1997). “Investigation of Variation in Swelling Pressure Values for an Expansive Soil.” *MS Thesis, Colorado State University, Fort Collins, Colorado*.
- Shah, F., Chao, K. C., and Soralump, S. (2023). “Evaluation of the Impact of Expansive Clay Heaving on Seepage and Stability of an Earth Dam.” *Proceeding of the 21st Southeast Asian Geotechnical Conference and 4th AGSSEA Conference, Bangkok, Thailand, October*.
- Skempton, A. W. (1953). “The Colloidal ‘Activity’ of Clays.” *Proceedings of the 3rd International Conference on Soil Mechanics and Foundation Engineering, Switzerland*, 1, 57–61.
- Soundara, B., Selvakumar, S., and Bhuvaneshwari, S. (2020). “Laboratory Study on Natural Fibre Amended Fly Ash as an Expansive Soil Stabilizer.” *Geotechnical Engineering Journal of the Southeast Asian Geotechnical Society and Association of Geotechnical Societies in Southeast Asia*, 51(4), December.
- Thompson, R. W., Perko, H. A., & Rethamel, W. D. (2006). “Comparison of Constant Volume Swell Pressure and Oedometer Load-Back Pressure.” *Proceedings of the 4th International Conference on Unsaturated Soils, Carefree, Arizona*, 1787-1798.
- Tian, X., Xiao, H., Li, Z., Li, Z., Su, H., and Ouyang, Q. (2022). “Experimental Study on the Strength Characteristics of Expansive Soils Improved by the MICP Method.” *Geofluid*, 1–10.